11 Terrain Analysis

Introduction

Elevation and related terrain variables are important at some point in almost everyone's life. Elevation and slope change across the landscape (Figure 11-1), and this variation determines where rivers flow, lakes occur, and floods are frequent. Terrain variation influences soil moisture and hence food production. Terrain in large part affects water quality through sediment generation and transport. Terrain strongly influences transportation networks and the cost and methods of building construction. Terrain

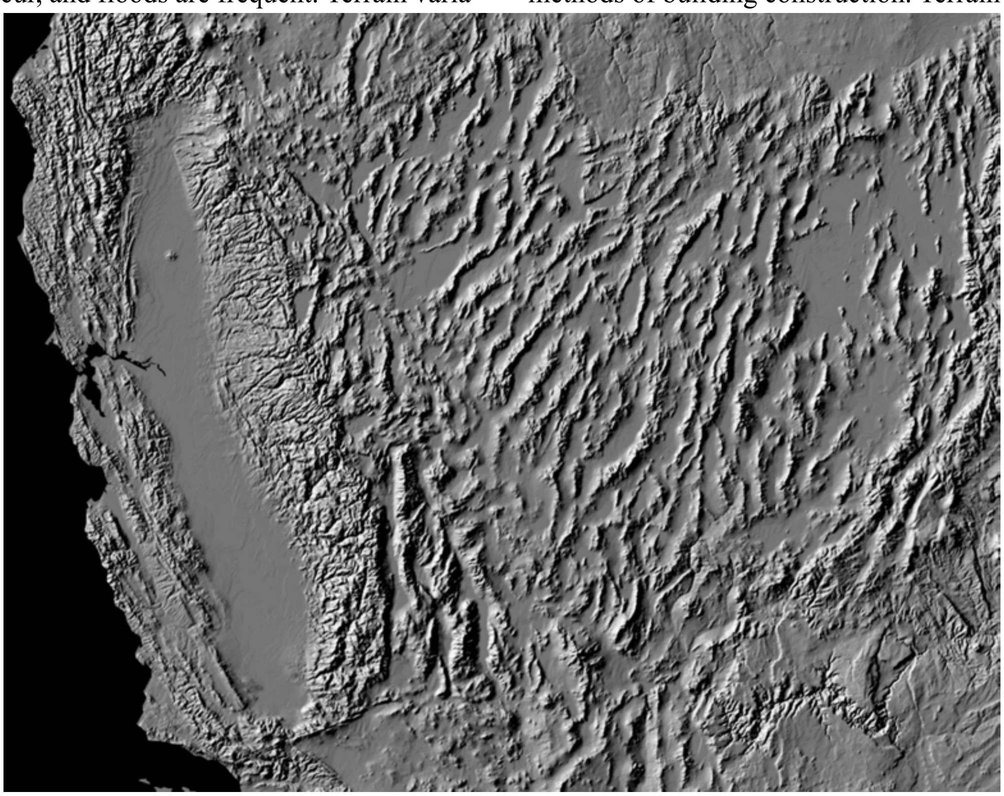

Figure 11-1: An example of a terrain-based image of the western United States. Shading, based on local elevation, emphasizes terrain shape. Topographic features are clearly identified, including the Central Valley of California at the left of the image, and to the center and right, the parallel mountains and valleys of the Basin and Range region (courtesy USGS).

variables are frequently applied in a broad range of spatial analyses (Table 11-1).

Given the importance of elevation and other terrain variables in resource management, and the difficulties of manual terrain analysis, it is not surprising that terrain analysis is well developed in GIS. Indeed, it is often impractical to perform consistent terrain analyses without a GIS. For example, slope calculations over large areas based on manual methods are slow, error prone, and inconsistent. Elevation change over a horizontal distance is difficult to measure, these measurements are slow, and estimates are likely to vary among human analysts. In contrast, digital slope calculations are easy to program, consistent, and have proven to be as accurate as field measurements.

Both data and methods exist to extract important terrain variables via a GIS. Digital elevation models (DEMs), described in Chapters 2 and 7, have been developed for most of the world using methods described in Chapters 5 and 6, and DEM renewal and improvement continues.

Table 11-1: A subset of commonly used terrain variables (adapted from Moore et al., 1993).

Variable	Description	Importance
Height	Elevation above base	Temperature, vegetation, visibility
Slope	Rise relative to horizontal distance	Water flow, flooding, erosion, travel cost, construction suitability, geology, insolation, soil depth
Aspect	Downhill direction of steepest slope	Insolation, temperature, vegetation, soil characteristics and moisture, visibility
Upslope area	Watershed area above a point	Soil moisture, water runoff volume and timing, pollution or erosion hazards
Flow length	Longest upstream flow path to a point	Sediment and erosion rates
Upslope length	Mean or total upstream flow path length from a point	Sediment and erosion rates
Profile curvature	Curvature parallel to slope direction	Erosion, water flow acceleration
Plan curvature	Curvature perpendicular to slope direction	Water flow convergence, soil water, erosion
Visibility	Site obstruction from given viewpoints	Utility location, viewshed preservation

Calculations are based on cell values assigned to a regular grid. We use the concept of Z values, the height stored in the raster arrays, to extract information about terrain, using the magnitudes and patterns of changes in Z across the grid (Figure 11-2). For example, the height differences between adjacent cells or in a neighborhood of cells are used to calculate a local slope (slope in Figure 11-2). The angle and orientation of lines defined by x, y, and Z values near a point are used to calculate the normal vector, at right angles to the local surface (Figure 11-2). Local curvature and slope direction are also calculated by differences in Z values in a neighborhood.

Many terrain analysis functions can be specified by a mathematical operation applied to an appropriate moving window. The results from these mathematical operations in turn provide important information about terrain characteristics that are helpful in spatial analysis.

Slope and Aspect

Slope and aspect are two commonly used terrain variables. They are required in many studies of hydrology, conservation, site planning, and infrastructure development, and are the basis for many other terrain analysis functions. Road construction costs and safety are sensitive to slope. Watershed boundaries, flowpaths and direction, erosion modeling, and viewshed determination (discussed later in this chapter) all use slope and/or aspect data as input. Slope or aspect may be useful in mapping both vegetation and soil resources.

Slope is defined as the change in elevation (a rise) with a change in horizontal position (a run). Seen in cross section, the slope is related to the rise in elevation over the run in horizontal position (Figure 11-3). Slope is often reported in degrees, between zero (flat), and 90 (vertical). The slope is equal to 45 degrees when the rise is equal to the run. The slope in degrees is calculated from the rise and run through the tangent trigonometric function. By definition, the tangent of the

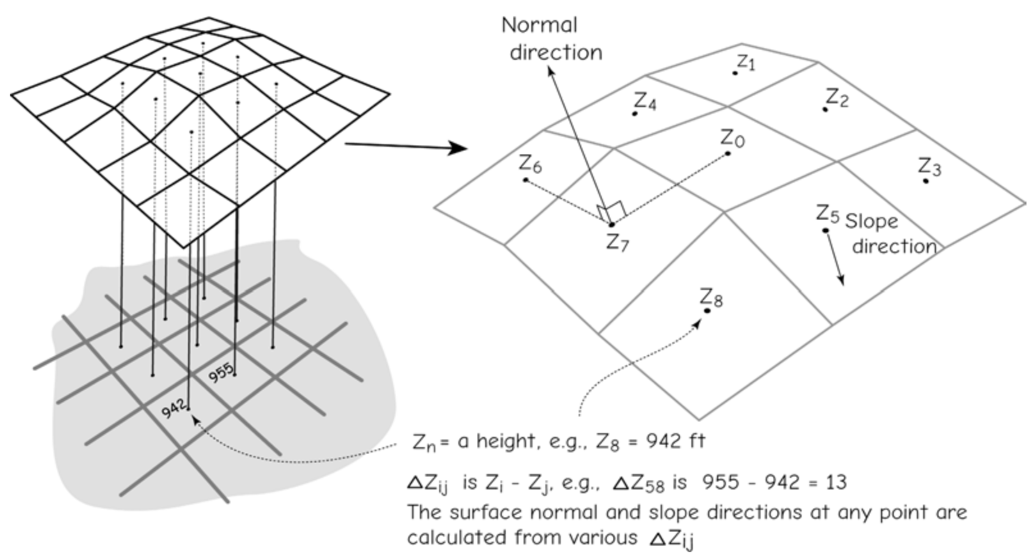

Figure 11-2: A depiction of a surface represented by a raster DEM, and changes in Z values for cells used for calculating various terrain attributes.

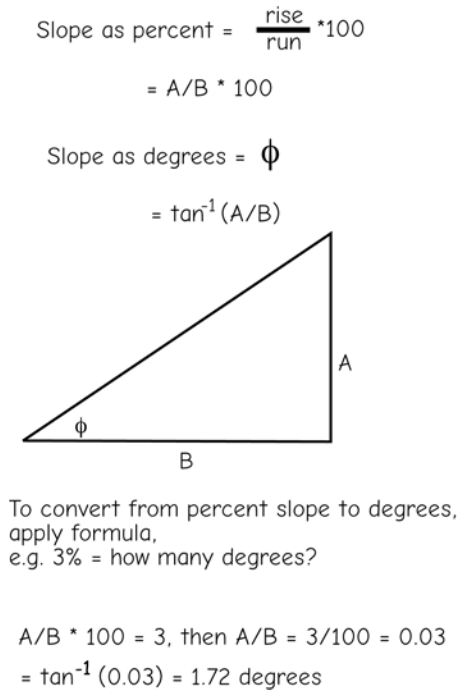

Figure 11-3: Slope formula, showing the rise (A), run (B), and slope angle (ϕ).

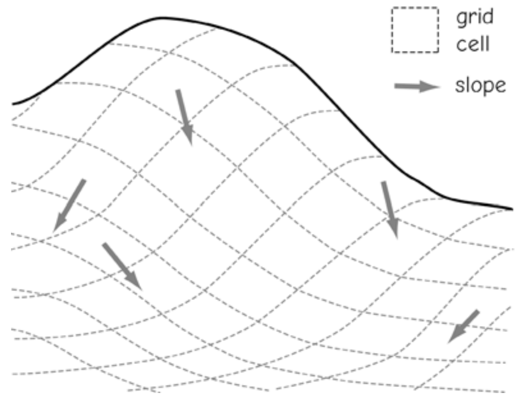

Figure 11-4: Slope direction, shown as gray arrows for some example locations above, often changes substantially among cells on a raster surface. Slope calculations in three dimensions require the consideration of all values surrounding a cell.

slope angle (ϕ) is the ratio of the rise over the run, as shown in (Figure 11-3). The inverse tangent of a measured rise over a run gives the slope angle. A steeper rise or shorter run lead to a higher ϕ and hence steeper slope.

Slope may also be expressed as a percent, calculated by 100 times the rise over the run (Figure 11-3). Slopes expressed as a percent have magnitudes from zero (flat) to infinite (vertical), with a sign convention inconsistently defined. Some authors define a positive slope as uphill (0 to +∞), and a negative slope downhill (0 to -∞), while others define slope only downhill (0 to +∞). A slope of 100% occurs when the rise equals the run.

Calculating slope from a raster data layer is more complicated than in the cross-section view shown in Figure 11-3. The raster cells occur at regular intervals across an irregular terrain surface. Slope direction at a point in the landscape is typically measured in the steepest direction of elevation change (Figure 11-4). Slope changes in a complex way across many landscapes, and calculations of slope must factor in the relative changes in elevations around a central cell.

As demonstrated in Figure 11-4, the slope direction often does not point parallel to the raster rows or columns. Consider the cells depicted in Figure 11-5. Higher eleva-

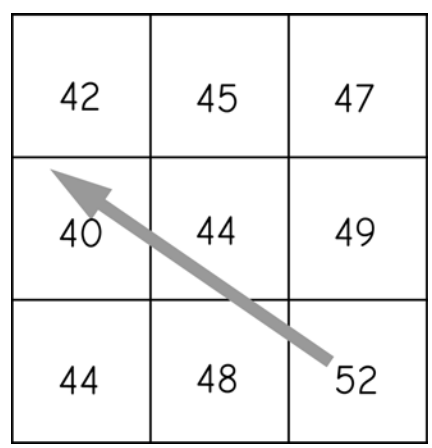

Figure 11-5: Slope direction on a raster surface usually does not point from cell center to cell center. Therefore, formulae that accurately represent slope on a surface integrate several cells surrounding the center cell.

tions occur at the lower right corner, and lower elevations occur toward the upper left. The direction of steepest slope trends from one corner towards the other, but does not pass directly through the center of any cell. How do we obtain values for the rise and run? Which elevations should be used to calculate slope? Intuitively we should use some combination of a number of cells in the vicinity of the center cell, perhaps all of them.

Elevation is often represented by the letter Z in terrain functions. These terrain functions are usually calculated with a symmetrical moving window. A 3 by 3 cell window is most common, although 5 by 5 and other odd-numbered windows are also used. Each cell in the window is assigned a subscript, and the elevation values found at window locations referenced by subscripted Z values.

Figure 11-6 shows an example of a 3 by 3 cell window. The central cell has a value of 44, and is referred to as cell Z_0. The upper left cell is referred to as Z_1, the upper center cell as Z_2, and so on through cell Z_8 in the lower right corner.

Slope at each center cell is most commonly calculated from the formula:

$$s = \operatorname{atan}\sqrt{\left(\frac{dZ}{dx}\right)^2 + \left(\frac{dZ}{dy}\right)^2} \qquad (11.1)$$

where s is slope, atan is the inverse tangent function, Z is elevation, x and y are the respective coordinate axes, and dZ/dx and dZ/dy are calculated for each cell based on elevation values surrounding a given cell. The symbol dZ/dx represents the rise (change in Z) over the run in the x direction, and dZ/dy represents the rise over the run in the y direction. These formulas are combined to calculate the slope for each cell based on the combined change in elevation in the x and y directions.

Many different formulas and methods have been proposed for calculating dZ/dx and dZ/dy. The simplest, shown in Figure 11-6 and at the top of Figure 11-7, use the four cells nearest to Z_0.

$$dZ/dx = (Z_5 - Z_4)/(2C) \qquad (11.2)$$

$$dZ/dy = (Z_2 - Z_7)/(2C) \qquad (11.3)$$

where C is the cell dimension and the Zs are defined as in Figure 11-6. This method uses the "four nearest" cells, Z_4, Z_5, Z_2, and Z_7, in calculating dZ/dx and dZ/dy. These four cells share the largest common border with the center. This four nearest method is perhaps the most obvious and provides reasonable slope values under many circumstances.

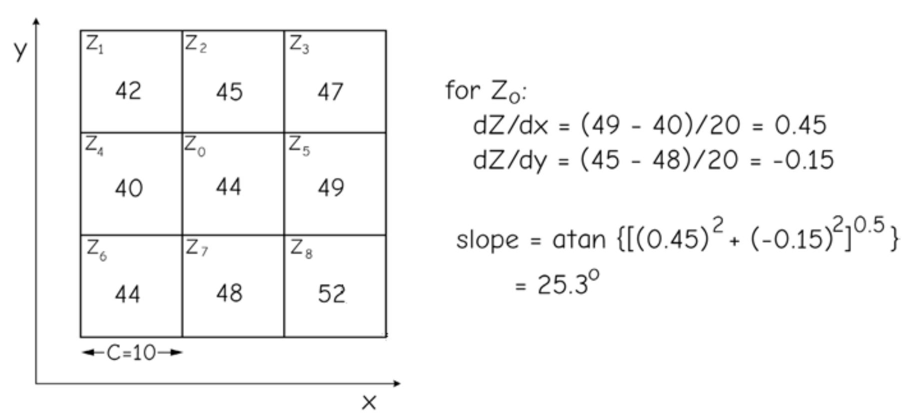

Figure 11-6: Slope calculation based on cells adjacent to the center cell.

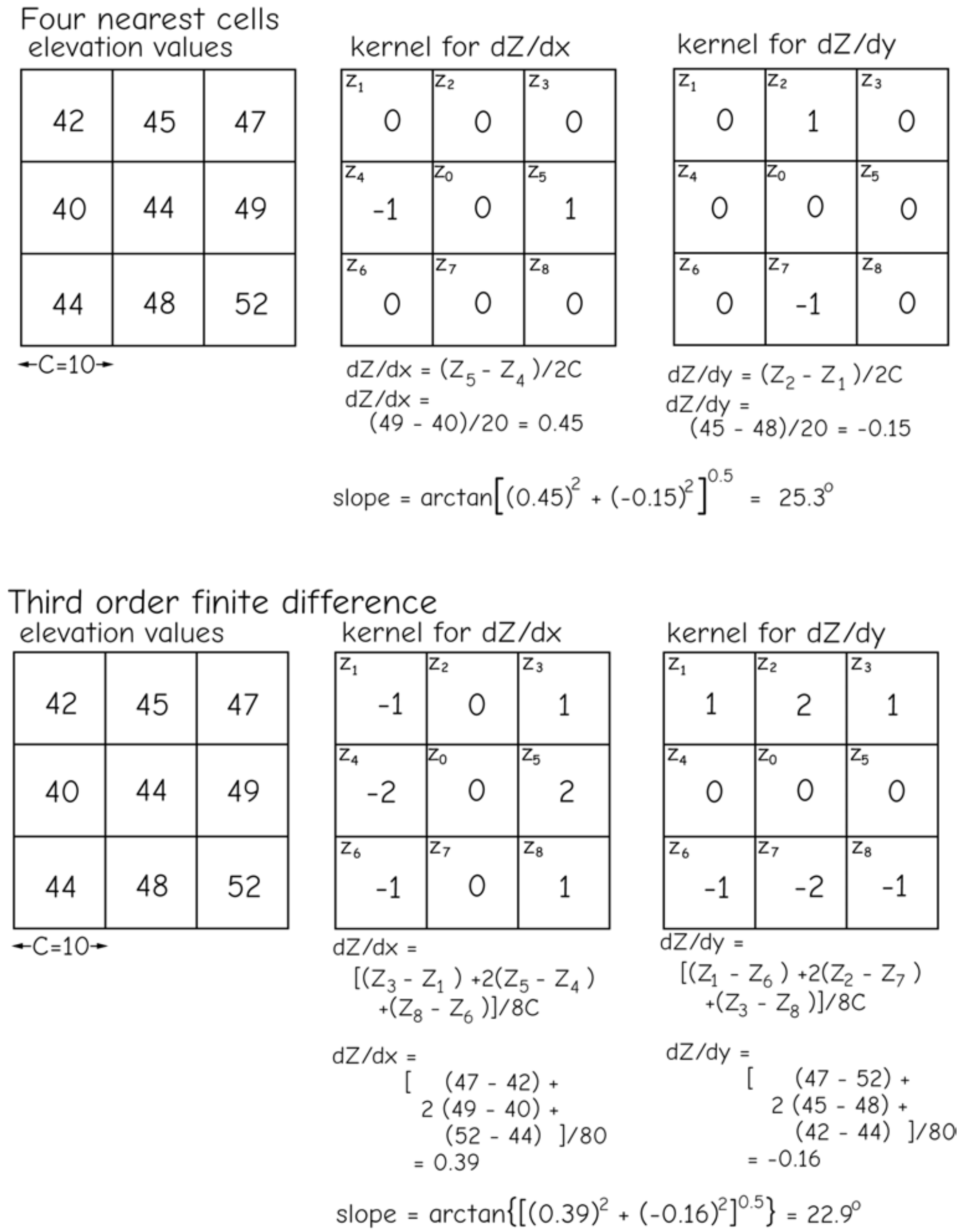

Figure 11-7: Four nearest cells method (top) and third order finite difference method (bottom, explained on the next page), used in calculating slope. C is cell size and dZ/dx and dZ/dy are the changes in elevation (rise) with changes in horizontal position (run). Note that different slope values are produced by the different methods.

A common alternate method is known as a *third order finite difference* approach (Figure 11-7, bottom). This method for calculating dZ/dx and dZ/dy differs mainly in the number and weighting it gives to cells in the vicinity of the center cell. The four nearest cells are given a higher weight than the "corner" cells, but data from all eight nearest cells are used.

Several other methods have been developed that are better for calculating slope under certain conditions. Better means that, on average, a method produces more accurate slope estimates when compared to carefully collected field measurements. However, no method has proved best under all terrain conditions. Literature on the methods, their derivation, and application are listed at the end of this chapter.

Comparative studies have shown the two methods described here to be among the best for calculating slope and aspect over a wide range of conditions. The method using the four nearest cells was among the best for smooth terrain, and the 3rd order finite difference approach is often among the best when applied to rough terrain.

Aspect is also an important terrain variable that is commonly derived from digital elevation data. The aspect at a point is the steepest downhill direction. The direction is typically reported as an azimuth angle, with zero in the direction of grid north, and the azimuth angle increasing in a clockwise direction (Figure 11-8). Aspects defined this way take values between 0 and 360 degrees. Flat areas have no aspect, because there is no downhill direction.

Aspect (α) is most often calculated using dZ/dx and dZ/dy:

$$\alpha = 180 - \mathrm{atan}\left(\frac{\left(\frac{dZ}{dy}\right)}{\left(\frac{dZ}{dx}\right)}\right) + 90\left(\frac{\left(\frac{dZ}{dx}\right)}{\left|\frac{dZ}{dx}\right|}\right) \qquad (11.4)$$

where atan is the inverse tangent function that returns degrees, and dZ/dy and dZ/dx are defined as above.

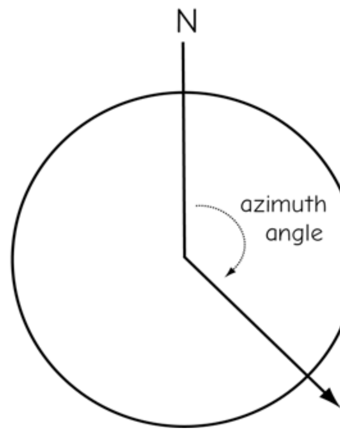

Figure 11-8: Aspect may be reported as an azimuth angle, measured clockwise in degrees from north.

As with slope calculations, estimated aspect varies with the methods used to determine dZ/dx and dZ/dy. Tests have shown the four nearest cell and third order finite difference methods again yield among the most accurate results, with the third order method among the best under a wide range of terrain conditions.

Profile curvature and *plan curvature* are two other local topographic indices that are important in terrain analysis and may be derived from gridded elevation data. Profile and plan curvature are helpful in measuring and predicting soil water content, overland flow, rainfall-runoff response in small catchments, and the distribution of vegetation.

Profile curvature is an index of the surface shape in the steepest downhill direction (Figure 11-9). The profile curvature may be envisioned by imagining a vertical plane, slicing downward into the earth surface, with the plane containing the line of steepest descent (aspect direction). The surface traces a path along the face of this plane, and the curvature is defined by the shape of this path. Smaller values of profile curvature indicate a concave (bowl shaped) path in the downhill direction, and larger values of profile curvature indicate a convex (peaked) shape in the downhill direction.

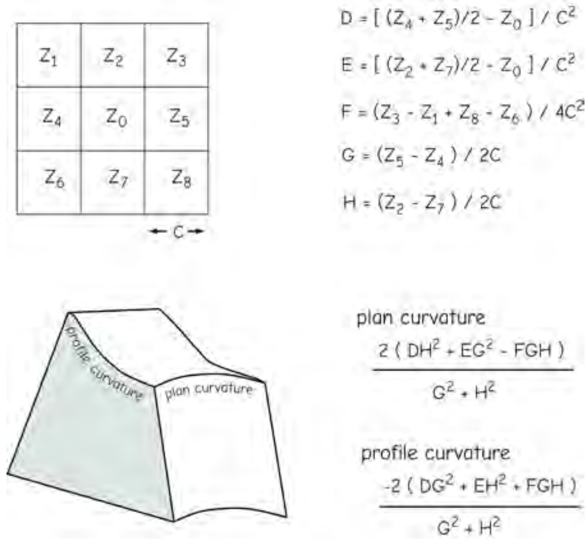

Figure 11-9: Profile curvature and plan curvature measure the local terrain shape. Formulas (left) combine values surrounding a center cell with coefficients that reveal concavity or convexity in the level (plan) and downhill (profile) directions (below).

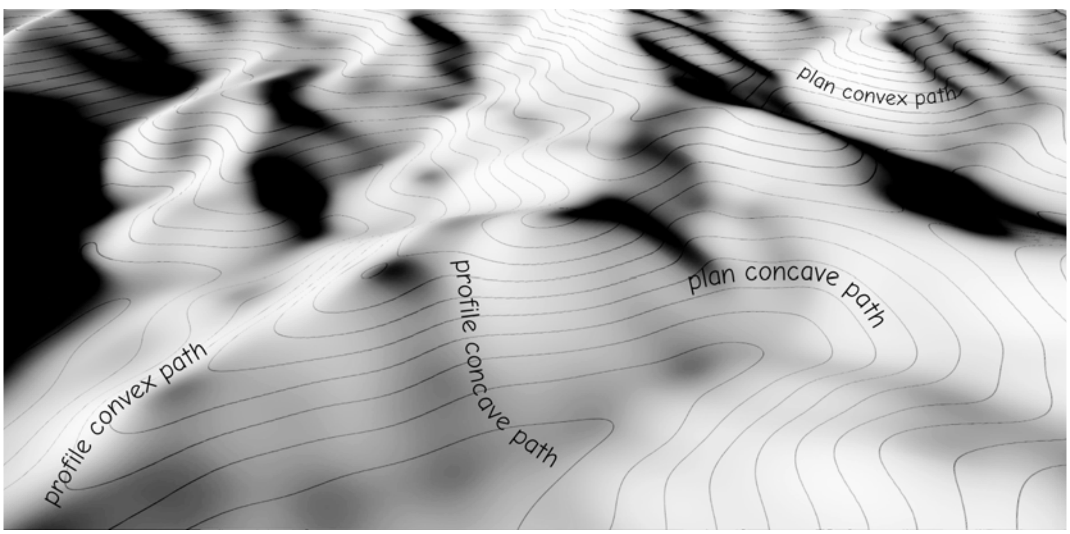

Different softwares apply different sign conventions, sometimes making concave curvature positive, sometimes assigning them negative values. Raw values are reported in some versions, while other softwares scale curvatures over a standard range, e.g., from 0 to 100. As with most spatial analysis, the specific software implementation should be verified over known test cases.

Plan curvature is the profile shape in the local direction of level, at right angle to the steepest direction. This means plan curvature is measured at a right angle to profile curvature (Figure 11-9). Plan curvature may also be envisioned as a vertical plane slicing into the surface, and is measured in a horizontal plane. The surface traces a path on the face of the plane, and the plan curvature is a measure of the shape of that path. Concave plan curvature values are small or negative for sloping valleys or clefts, while convex plan curvature values at ridge and peak sites are large or positive.

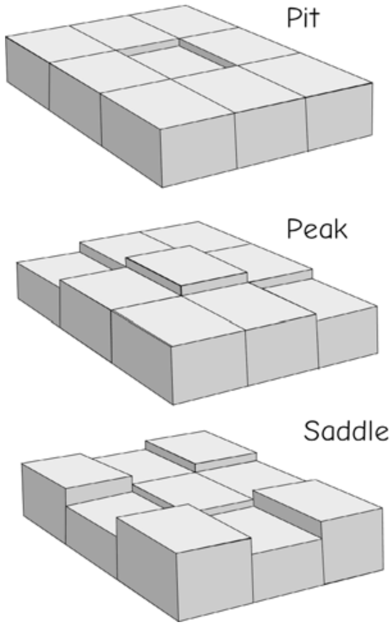

Figure 11-10: Morphometric feature types may be defined by the relative heights, and hence directional convexity, of adjacent cells (adapted from Jo Wood, 1996).

These concepts of directional terrain shape may be developed further to identify *terrain* or *morphometric features*. These are characteristic terrain elements including planes, peaks, passes, saddles, channels, ridges, shoulders, toe slopes, and pits (Figure 11-10). Each of these shapes has particular terrain attributes that often affect important spatial variables. For example, soil is thinner and water scarcer on ridges and peaks because they are convex, while materials accumulate in pits and channels.

Terrain features may be identified by observing the convexity in the plan and profile directions. For example, peaks are characterized by convex shapes in both the x and y directions, a ridge is convex in one direction but relatively flat in another, while a pit is concave in orthogonal directions (Figure 11-10). Formulas similar to those in Figure 11-9 have been developed to measure the convexity and concavity in specified orthogonal directions. The various combinations may then be applied to identify terrain features (Figure 11-11).

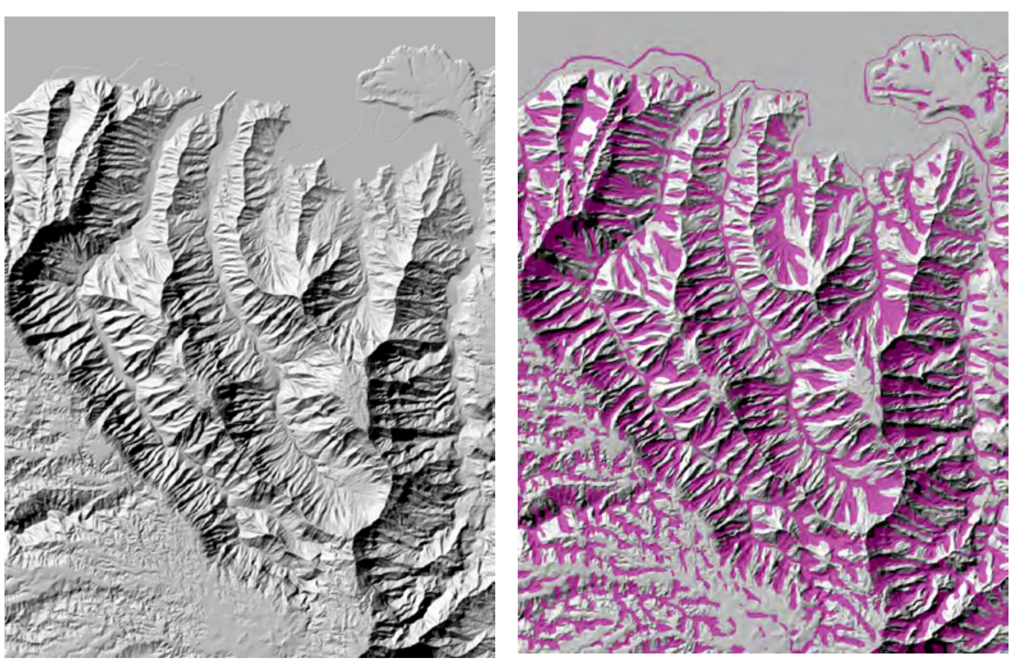

Figure 11-11: Terrain morphometery, or morphometric features may be derived from directional convexity measures. A shaded map of a mountainous area shows valleys and channels (above, left), which are identified via morphometric terrain analyses and shown as uniformly shaded areas (above, right).

Hydrologic Functions

Digital elevation models are used extensively in hydrologic analyses. Water is basic to life, commerce, and comfort, and there is a substantial investment in water resource monitoring, gathering, protection, and management. Spatial functions are applied to DEMs to yield important information on hydrology.

A *watershed* is an area that contributes flow to a point on the landscape (Figure 11-12). Watersheds may also be named basins, contributing areas, catchments, drainages, and subbasins or subcatchments. The entire uphill area that drains to any point on a landscape is the watershed for that point. Water falling anywhere in the upstream area of a watershed will pass through that point. Watersheds may be quite small. For example, the watershed may cover only a few square meters on a ridge or high slope. Local high points have watersheds of zero area because all water drains away. Watersheds may also be quite large, including continental areas that drain large rivers such as the Amazon or Mississippi Rivers. Any point in the main channel of a large river has a large upstream watershed.

The *drainage network* is the set of streams and rivers in a watershed, and it is completely contained within the watershed. As shown in Figure 11-12, the stream network often shows a dendritic pattern, with smaller watercourses branching off from larger segments as one moves upstream. The base of the drainage network is often called a *pour point* or *outlet*.

Flow direction is used in many hydrologic analyses. The true surface flow direction is the path water would take, if dumped in sufficient excess on a point so as to generate surface flow. This excess water flows in the steepest downhill direction, usually set equivalent to the local aspect.

The use of aspect to assign flow direction may be wrong, particularly in nearly flat areas and in built environments. Water flows both above and below the surface; if subsurface flow is large, ignoring it may cause errors. If soils have different permeabilities, or resistance to flow, then subsurface flow direction may be different than surface flow direction. In steep, undeveloped terrain, there is a strong downslope gravitational gradient that often dominates, and surface and subsurface flow directions are often similar, so aspect provides a reasonable approximation of overall flow direction. In flat or nearly flat terrain, soil permeability may dominate, causing different subsurface and surface flow directions. Ditches, culverts,

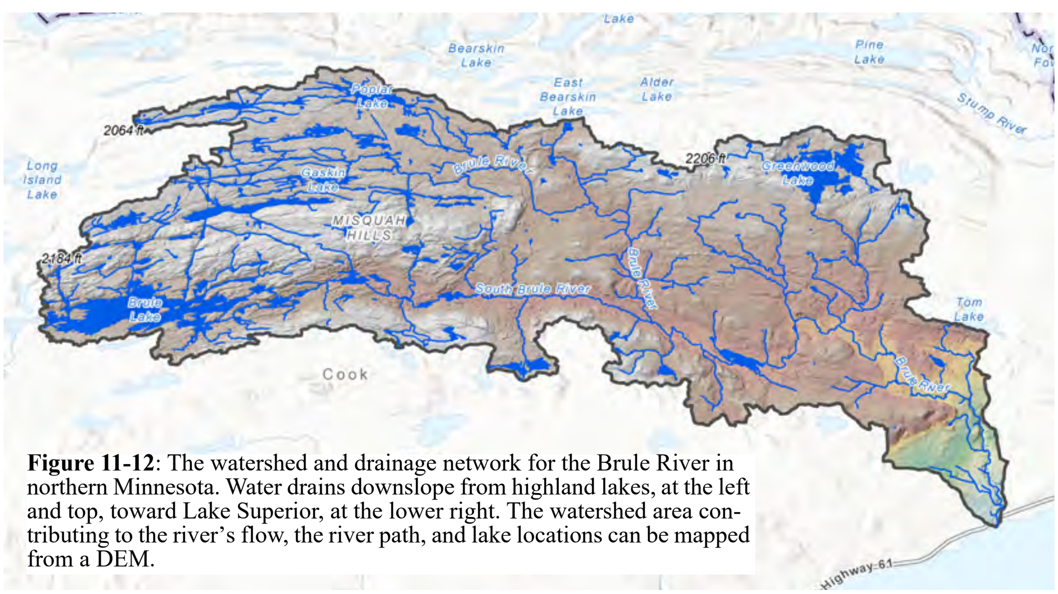

Figure 11-12: The watershed and drainage network for the Brule River in northern Minnesota. Water drains downslope from highland lakes, at the left and top, toward Lake Superior, at the lower right. The watershed area contributing to the river's flow, the river path, and lake locations can be mapped from a DEM.

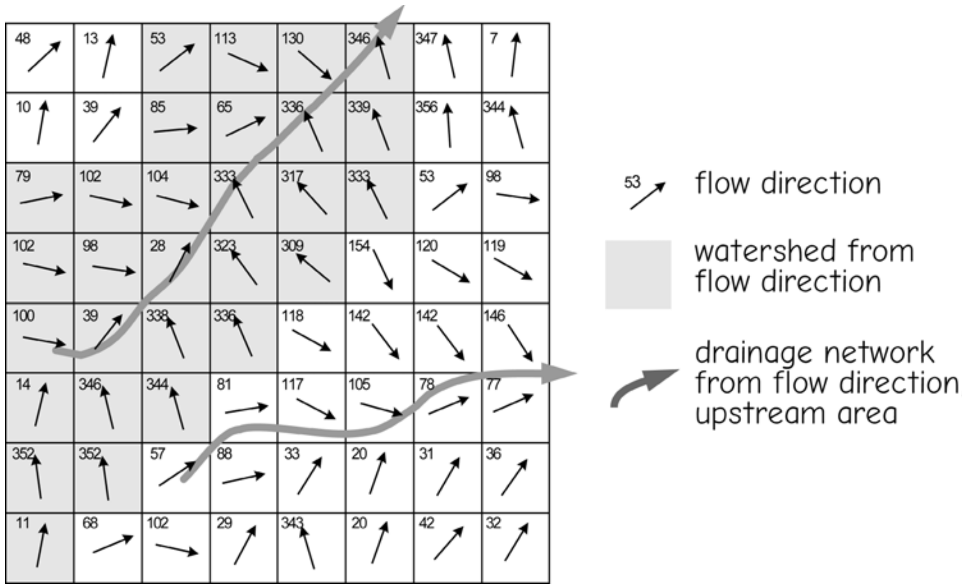

Figure 11-13: Flow direction (arrow, and number reflecting azimuth degrees), watershed, and drainage network shown for a raster grid. Elevation data are used to define the flow direction for each cell. These flow directions are then used to determine a number of important hydrologic functions.

buried storm sewers, and other built features alter flow directions in ways that aren't represented by terrain. However, subsurface drainage and built features are often based on modified flow directions that are first derived from surface shape.

Flow directions may be envisioned as an arrow from a single cell to a single adjacent cell, and stored as compass angles in a raster data layer (Figure 11-13). Acceptable values are from 0 to 360 if the angle is expressed in degrees azimuth. Alternately, flow direction can be stored as a number indicating the adjacent cell to which water flows, taking a value from 1 to 8 or some other unique identifier for each direction towards cells.

The use of a single flow direction is an incomplete representation in many instances. Cells often exhibit divergent flow, in multiple directions out of a cell to multiple adjacent cells (Figure 11-14). Flows may also be convergent, with multiple cells contributing to a cell. The most common flow direction methods provide a single direction for each cell, so divergent and some convergent flows are not represented. One solution involves recording sub-cell flow directions, but this leads to more complicated raster structures and calculations.

When the flow direction arrow from one cell does not point exactly at the adjacent cell, we may distribute the flow to more than one adjacent cell. There are various ways to distribute flows among adjacent cells. The *D8* method is common, and assigns all flow from a cell to the cell with the steepest

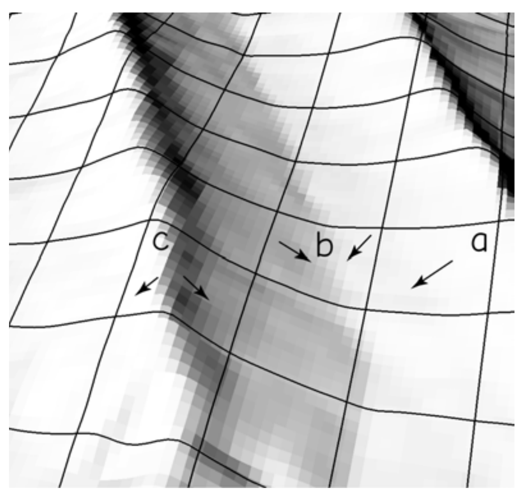

Figure 11-14: An example of simple (a), convergent (b), and divergent (c) flow.

downhill gradient (Figure 11-15, left). The D8 is simple to understand, program, and store, but is particularly poor at representing divergent flow and flow in low-gradient areas. This can cause large errors in derived measures such as upslope contributing area or soil moisture indexes, and lead to atypical drainage networks in nearly flat areas. Output flow direction rasters derived from the D8 method may be represented with only 8 codes, allowing a simple and compact data layer.

Alternative flow direction methods may assign flow to multiple cells, and hence represent some forms of divergent flow. One common method, known as *D-infinity*, distributes flow to one downslope cell when the flow direction is exactly toward the center of the cell, and otherwise assigns a portion of the flow to each of the two adjacent cells in the downslope direction (Figure 11-15, right). The split is proportional to the angles between the steepest downslope direction and the respective cell centers. This reduces the main shortcoming of the D8 method, while slightly increasing complexity.

While perhaps more accurate in many conditions, multiflow direction systems have not been widely implemented. A more common option is to use higher-resolution raster data such that raster cell size is small enough to make within-cell divergence or convergence impacts negligible

Flow accumulation area, contributing area, or *upslope area* are other important hydrologic characteristics. A flow accumulation area function is based on a flow direction surface. The flow accumulation function places a value in each cell that is the area uphill that drains to that cell.

Watersheds may be identified once a flow direction surface has been determined. Flow direction is followed "uphill" from a point, until a peak is reached. Each uphill cell may have many contributing cells, and the flow into each of these cells is also followed uphill. The uphill list is accumulated recursively until all cells contributing to the starting cell have been identified, and thus the watershed is defined.

Flow direction in flat areas is difficult to calculate and prone to error. Aspect is undefined in a truly flat region, because there is zero gradient. Flow directions in these cases may be strongly influenced by small height errors, so flow directions are sometimes

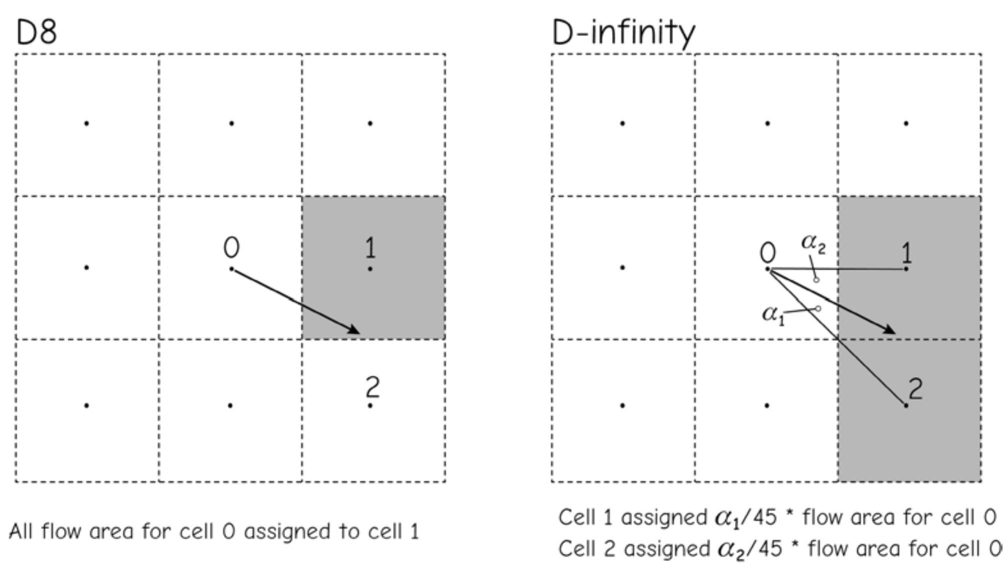

Figure 11-15: The D8 flow direction method (above left) assigns all flow to the cell center closest to the flow direction (cell 1), while the D-infinity method partitions the flow to the two cells nearest the flow direction, proportional to the flow direction angles (cells 1 and 2, above right).

manually specified, or the aspect calculated using a larger cell size or neighborhood. The neighborhood may be successively expanded until an unambiguous flow direction is defined.

Vector incision is another common method for prescribing flow direction in flat areas. A vector flowpath, e.g., a digitized stream segment, is overlain with the raster, and raster values modified downstream along the vector to specify an appropriate flow direction. The most common approach lowers elevations along the flowpath, taking care to not create a sink along or at the end of the flowpath.

A *drainage network* is the set of cells through which surface water flows. Streams, creeks, and rivers occur where flow directions converge. Thus, a flow direction may be used to produce a map of likely stream location, prior to field mapping a stream (Figure 11-13, Figure 11-16). A drainage network may be defined as any cell that has a contributing uphill area larger than some threshold. These drainage networks are only approximations, because the method does not incorporate soil texture, depth, porosity, subsoil water movement, or other properties that affect surface flow. Nonetheless, a drainage network derived from terrain data alone is often a useful first approximation. The uphill area for each cell may be calculated, and the area compared to the threshold area. The cell is marked as part of the drainage network if the area surpasses the threshold.

A drainage network may have discontinuous lines when local small dams or sink areas capture flow, where all surrounding cells point into, and none out of, a location (Figure 11-16). This may create cells immediately downhill from the sink that has a zero

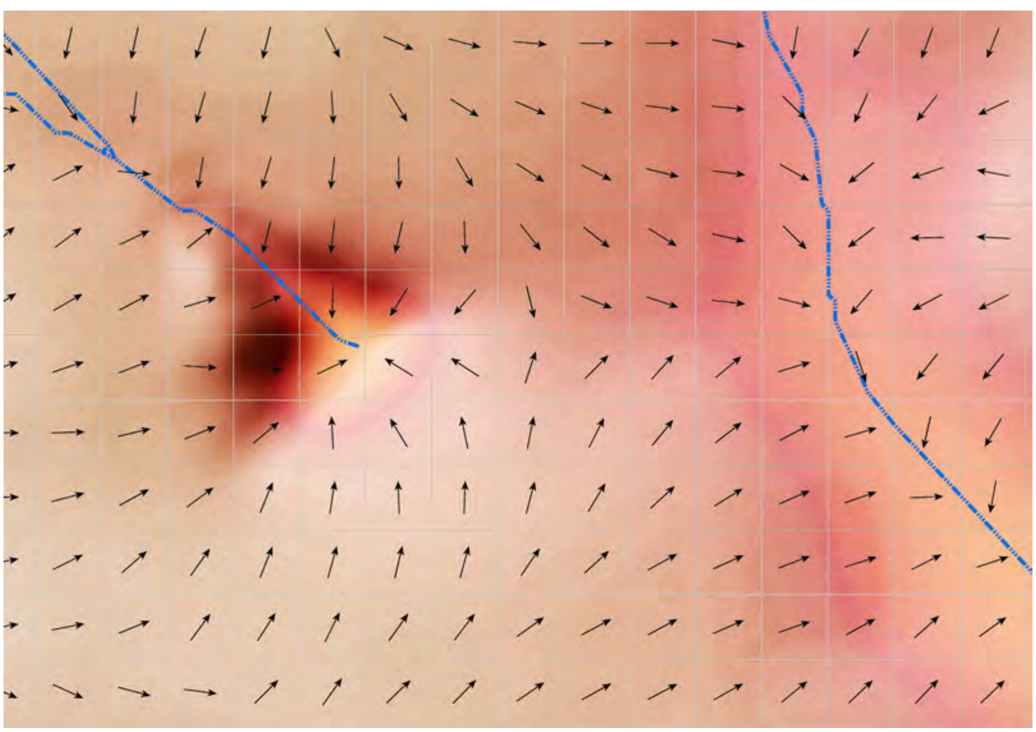

Figure 11-16: Flow direction (black arrows) calculated over a surface. The right side shows a flowline (dotted, blue in electronic edition) along a convergent zone, with values above the surface accumulation threshold. On the left of the figure is a local sink, with all flow directions pointing inward. The flowline from the upper left enters the sink and does not exit.

upstream area. The stream will end, but then may begin again further downhill. Natural sinks may be quite common in *karst* regions. where sinkholes occur on the surface due to collapsed subterranean caverns (Figure 11-17). Hydrologic sinks are also common along drainage ways in dry areas where check dams are built to reduce flash flooding or store water. Pits are also common in areas of deranged topography, for example, in the relatively flat, recently glaciated terrain. In most other areas, pits are often data artifacts and do not represent real geography. Pits represented in DEMS should be evaluated earlier during processing to determine if they are real, and how processing alters results.

Random errors in DEM elevation values often create spurious *pits* (also known as *false sinks)*. Because our technologies for creating DEMs are imperfect, DEMs often contain these pits that aren't on the Earth's surface.

Spurious pits are found in most DEMs due to small elevation errors. For example, DEM data collected with LiDAR often have a small ground footprint, and may sample small features that are above the surrounding ground level. A laser image over a recently plowed field may return spot heights for local mounds and furrows, incompletely harvested crops, and farm machinery. A log or dense shrubs in a steep-sided ravine may be misidentified as the ground surface, creating a barrier in the data that doesn't represent true conditions. Pits can be artifacts of interpolation methods that are used to fill in the grid values in unsampled locations. Post processing aims to remove these spurious readings, but they are common nonetheless.

Pits may cause problems over locally flat surfaces, often along drainage ways (Figure 11-18). Flow direction and flow accumulation functions often return errors due to spurious pits, particularly near watercourses. These low areas are shown as white patches in the figure. These apparent ponds do not exist in many landscapes, in that an erroneous pit in a stream course creates false basins.

Pits causes errors in subsequent hydrologic calculations. Drainage networks are incomplete, flow accumulation values are too low, and watersheds may be improperly identified when pits are encountered (Figure 11-19).

Figure 11-17: Examples of a discontinuous stream network, with downslope flow stopping at a sink (A), and then restarting downhill (B) when the flow accumulation threshold is again surpassed. The same kind of break is observed at a road crossing (C and D), although there is likely a culvert, not represented in the DEM.

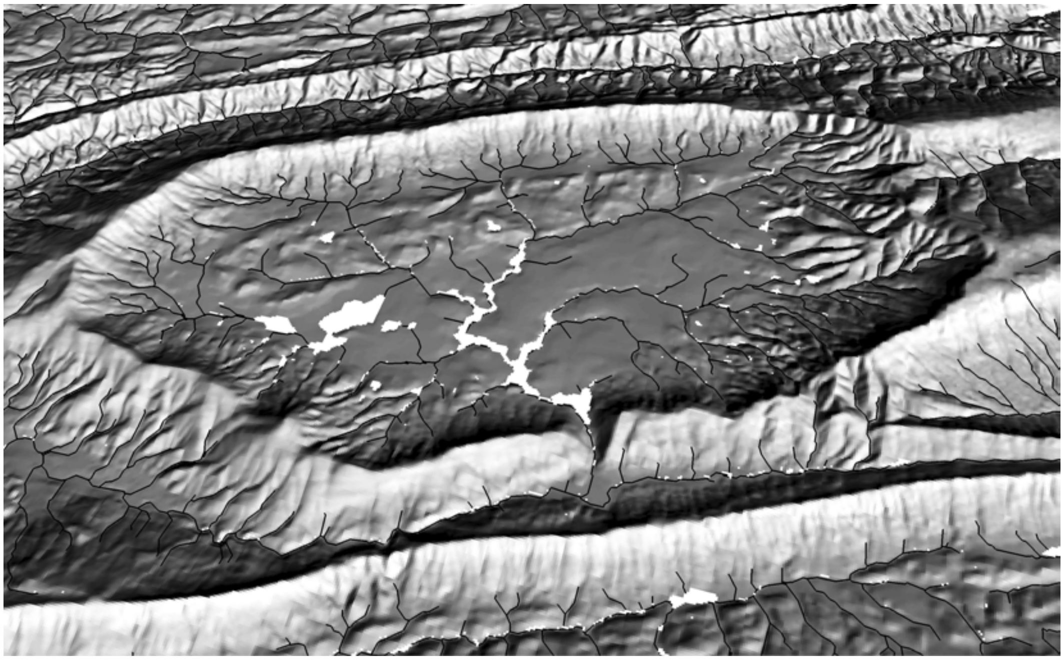

Figure 11-18: Examples of erroneous pits caused by DEM errors. The light-colored areas along drainage ways show local depressions that are artifacts of data errors, and don't exist on the landscape. Drainage networks and watersheds based on unfilled DEMs will be in error, because the flow directions based on the DEMs will be inward at all pits.

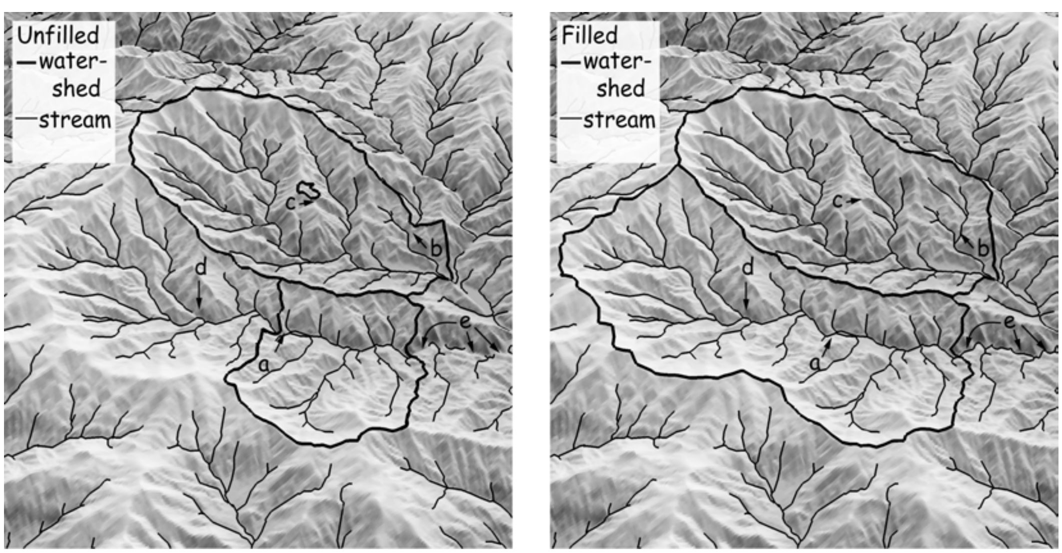

Figure 11-19: Watersheds and stream networks delineated from unconditioned DEMs (above, left) often result in missing stream segments, shown at a, b, d, and e, and incomplete watersheds (upstream from a and b, and at c).

DEMs must be "conditioned" to remove erroneous depressions (Figure 11-20). This involves pit identification, followed by either filling or downcutting downstream cells to remove the pit. A threshold is often specified above which a pit is not removed. This threshold is typically larger than common vertical errors in the data but also less than any true, "on the ground," pit depth. Known pits may be identified prior to the filling process and left unfilled. Once spurious pits are removed, further processing to identify watersheds and drainage networks may proceed.

The pit may substantially alter the DEM, and the scope of alteration may depend on the method (Figure 11-21). A fill process raises the values of a local depression until all cell values are at least equal to the value at the local "rim" or edge of the depression (Figure 11-21, center). This may create a flat surface, with no unambiguous drainage direction, so some variants of the fill process add a small slope over large fill areas to ensure drainage toward a downhill direction. Pits may also be removed through a breaching process (Figure 11-21, bottom), in which cells along a steepest gradient are lowered, searching a specified surrounding area to identify the steepest downhill path.

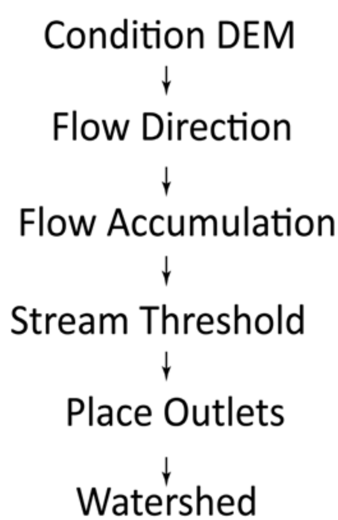

Figure 11-20: Steps in a watershed delineation.

As shown in Figure 11-21, breaching may sometimes better reflect the true drainage pathways rather than fills, and may result in more "natural" landscapes. It often depends on the nature of the depression, whether it is due to a spurious, small, isolated low elevation value (fill usually preferred for conditioning), or a narrow, high, linear feature, often built and with a culvert or other subsurface drainage way (breach usually preferred for conditioning). Unfortunately, many GIS softwares do not provide a breach function, even though breaching is increasingly useful for high-resolution DEMs based on LiDAR over urban or built-up areas.

Drainage and watershed geography inferred from terrain analysis depend substantially on the algorithm used, particularly for flow direction, so care should be taken in identifying the methods and thresholds that give sufficiently accurate results for the intended tasks. Many softwares only provide depression filling, and D8 flow direction, and often result in erroneous flowpaths in flat or near-flat terrains. The broadest range of general hydrologic and general terrain analysis tools are currently provided by Whitebox GAT, developed and maintained by John Lindsay at the University of Guelph.

To review, the steps for identifying a watershed from a DEM is shown inFigure 11-22. DEMs are conditioned as needed, and then the flow direction, accumulation, stream threshold, and watershed boundaries calculated. Different conditioning and flow accumulation methods may result in slightly different stream locations and, in some cases, watershed boundaries.

Several other hydrologic indices have been developed to identify locally convergent or divergent terrain positions, or terrain morphometry related to hydrography. These indexes are used in many subsequent topographic and hydrologic analyses, such as predicting plant community composition or growth, erosion modeling, or estimating the rainfall required to saturate an area and predict the likelihood and intensity of flooding.

Figure 11-21: A DEM (top) with large sinks at A through D as a result of highway berms, with several smaller sinks in other locations. Sinks are removed by either a fill process (middle), or breaching (bottom). Breaching results in an output surface that is more accurate for most applications.

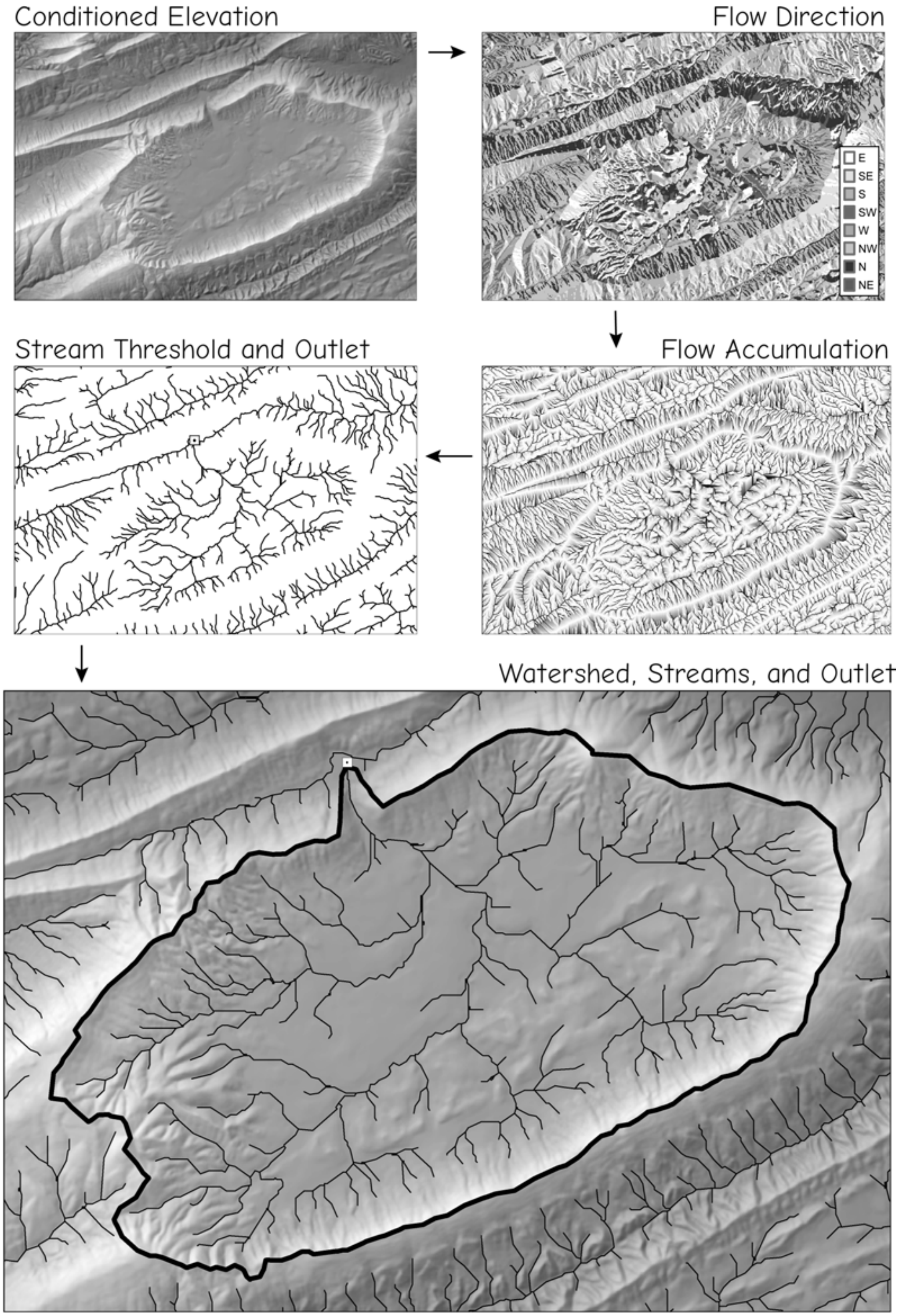

Figure 11-22: An example of the steps required to create watershed and drainage network features from a digital elevation model.

The *specific catchment area* (SCA) is defined as the total area draining to a point relative to drainage width, in raster data sets calculated as

$$SCA = AREA/C \qquad (11.5)$$

where AREA is the accumulated surface area upstream from a point, and C is the raster cell dimension. *Stream power index* (SPI) is defined as:

$$SPI = SCA * \tan(b) \qquad (11.6)$$

where b is the slope at a point, and SCA is as defined above. SPI is used to identify the potential erosion at a point, which depends both on the upstream area and hence ability to accumulate water, and the local slope, which drives the erosive energy in water flow.

Perhaps the most commonly applied wetness index is calculated by:

$$w = \ln\left(\frac{SCA}{\tan\beta}\right) \qquad (11.7)$$

where w is the wetness index at a cell, SCA is the specific catchment area, and β is the slope at the cell. This index has been shown to effectively represent the increased soil wetness due to large upslope areas and low slopes, particularly when combined with plan curvature and profile curvature measurements. These factors sort terrain along ridge-to-stream and convex-to-concave gradients.

There are many other topographic indices, e.g., for estimating total solar radiation, surface air drainage, or surface roughness. These and others are described in the references at the end of this chapter.

Contour Lines

Contour lines, or topographic contours, are connected lines of uniform elevation that run at right angles to the local slope. Contour lines are a common feature on many map series; for example, they are depicted on the USGS 1:24,000 scale nationwide series, and Britain's 1:50,000 Ordinance Survey maps. The shape and density of contour lines provide detailed information on terrain height and shape in a two-dimensional map, without the need for continuous tone shading. Both color and continuous tone printing were important limitations for past cartographers. Contour lines could be easily drawn with simple drafting tools. Although continuous tone printing is much less expensive today, contours will remain common as they have entered the culture of map making and map reading.

Several rapid, efficient methods have been developed for calculating contours, either from points or from grid data (Figure 11-23). Early contour maps and DEMs were developed from height measurements at a set of points. While useful, these points did not provide clear depictions of elevation. Contour lines of fixed values were interpolated

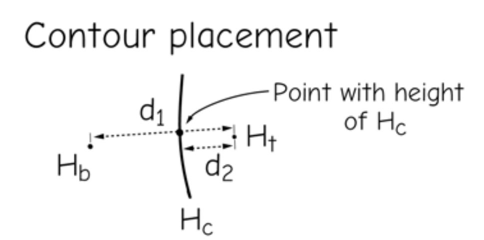

$$d_2 = d_1 \cdot \frac{H_t - H_c}{H_t - H_b}$$

Figure 11-23: Contour line locations are often estimated from point height locations, as a linear proportion of the height and distance differences between points.

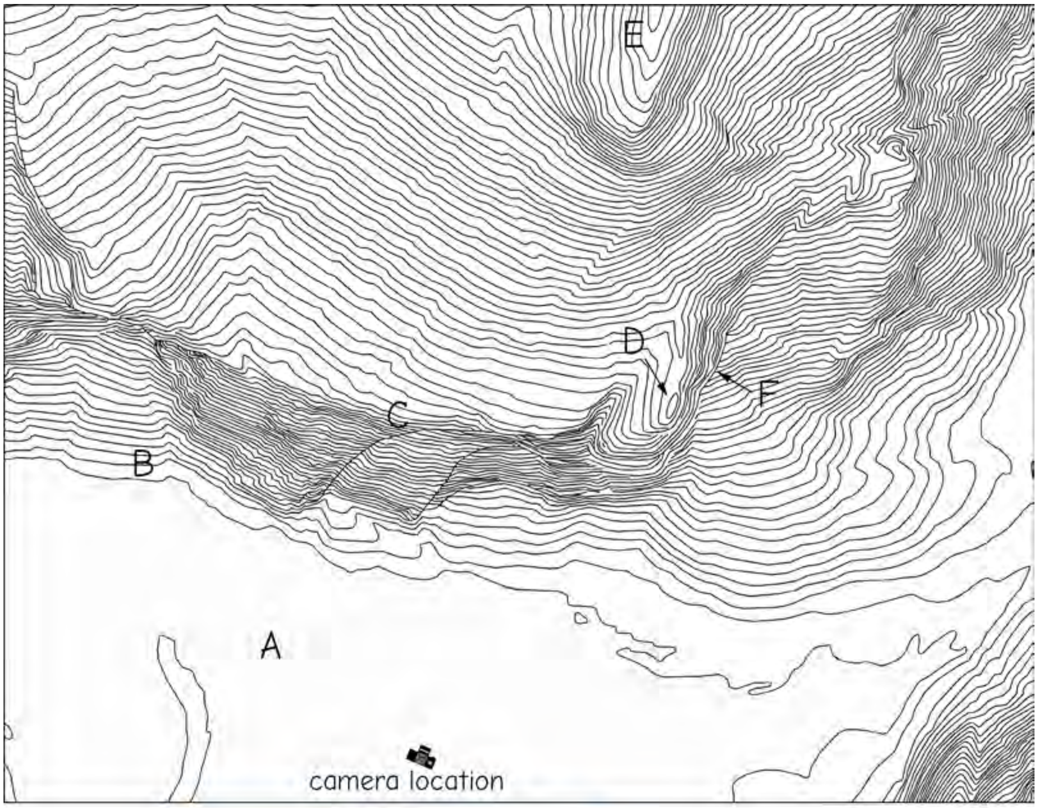

Figure 11-24: Contours may depict terrain features succinctly, as shown in this contour map, looking vertically downward on the area approximately shown in the photo. The image includes the Royal Arches and North Dome, from Yosemite Valley, California. Changes in slope, cliffs, overhangs, and peaks are all succinctly represented by contour lines.

linearly between nearest measurement points, as shown in Figure 11-23. Later measurement methods either identified contour lines directly from stereopairs (see Chapter 6), or derived them from mechanically or electronically produced rasters. Raster to contour generation also typically follows a linear interpolation. For a raster, appropriate adjacent cell centers are selected, and contour values interpolated as illustrated in Figure 11-23.

Contour lines are typically created at fixed height intervals, for example, every 30 m (100 ft) from a base height (Figure 11-24). Because each line represents a fixed elevation above or below adjacent lines, the density of contour lines indicates terrain steepness. Point A in Figure 11-24 falls in a flat area (the foreground of the photo, at bottom), where elevation does not change much, and there are few contour lines. Steep areas and cliffs are depicted by an increase in contour density, as shown at point B, with changes in steepness depicted by changes in density (above and below point C). Peaks, such as the top of Washington's column, D, and North Dome, E, appear as concentric rings. Note that contours may succinctly represent complex terrain structures, such as the curving arches in the center of the photograph, and shown below point C, and the overhanging cliff, to the left of point F.

Profile Plots

Profile plots are another common derivative of elevation data. These plots sample elevation along a linear *profile path*, and display elevation against distance in a graph (Figure 11-25). Elevation is typically plotted on the y axis, and horizontal distance on the x axis These profile plots are helpful in visualizing elevation change, slope, and cumulative travel distance along the specific profile path. Profile plots are common on the edges of maps, particularly maps of off-road, bicycle, or cross-country routes.

Profile plots often have some level of vertical exaggeration because horizontal distances are usually much larger than elevation gain. Vertical exaggeration is a scaling factor applied to the elevation data when shown on the graph. For example, Figure 11-25 shows a square graph that depicts approximately 31 km across the Earth's surface. The vertical elevation axis spans approximately 2.5 km over the same dimensions on the graph. This is a vertical exaggeration of approximately 12 (from 31/2.5).

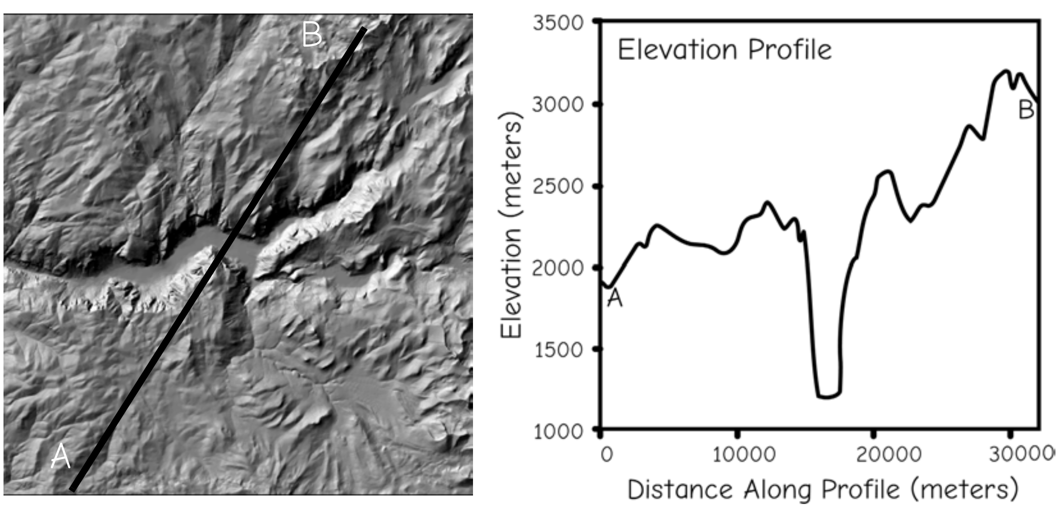

Figure 11-25: An example of a profile plot. The profile path is shown on the shaded relief image (left), with the starting point A and ending point B. The profile plot is shown on the right, with corresponding starting and ending points. The plot shows the change in elevation along the path. Note that the vertical exaggeration here is approximately 9 to 1.

Viewsheds

The *viewshed* for a point is the collection of areas visible from that point. Views from many locations are blocked by terrain. Elevations will hide points if the elevations are higher than the line of sight between the viewing point and target point (Figure 11-26).

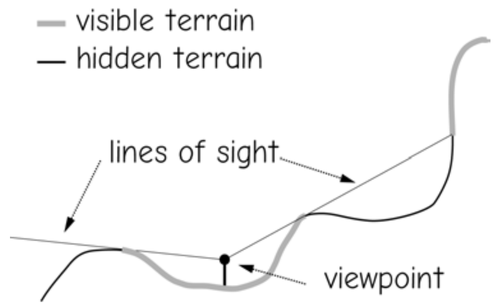

Figure 11-26: Mechanics of defining a viewshed.

Viewsheds and visibility analyses are quite important in many instances. High-voltage power lines or cell towers are often placed after careful consideration of their visibility, because most people are averse to viewing them. Communications antennas, large industrial complexes, and roads are often located at least partly based on their visibility, and viewsheds are specifically managed for many parks and scenic areas.

A viewshed is calculated based on cell-to-cell intervisibility. A line of sight is drawn between the view cell and a potentially visible target cell (Figure 11-26). The elevation of this line of sight is calculated for every intervening cell. If the slope to a target cell is less than the slope to a cell closer to the viewpoint along the line of sight, then the target cell is not visible from the viewpoint. Specialized algorithms have been developed to substantially reduce the time required to calculate viewsheds, but in concept, lines of sight are drawn from each viewpoint to each cell in the digital elevation data. If there is no intervening terrain, the cell is classified as visible. The classification identifies areas that are visible and areas that are hidden (Figure 11-27). Viewsheds for line or area features are the accumulated viewsheds from all the cells in those features.

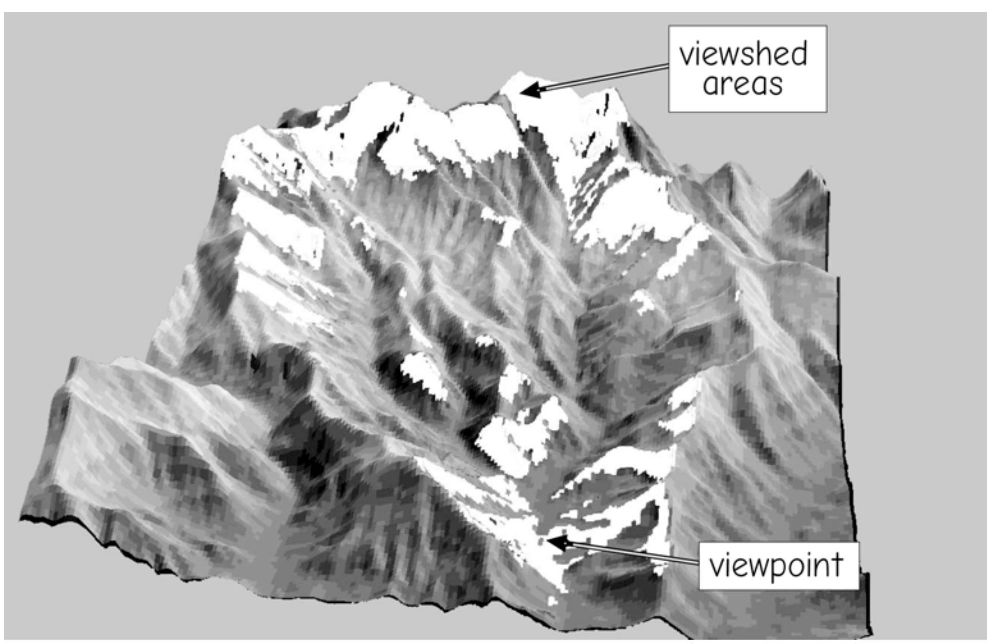

Figure 11-27: An example of a viewpoint, and corresponding viewshed.

Shaded Relief Maps

A *shaded relief map*, also often referred to as a *hillshade map*, is a depiction of the brightness of terrain reflections given a terrain surface and sun location. Although shaded relief maps are rarely used in analyses, they are among the most effective ways to communicate the shape and structure of terrain features, and many maps include relief shading (Figure 11-28).

Shaded relief maps are developed from digital elevation data and models of light reflectance. An artificial sun is "positioned" at a location in the sky and light rays projected onto the surface depicted by the elevation data. Light is modeled that strikes a surface either as a direct beam, from the sun to the surface, or from background "diffuse" sunlight. Diffuse light is scattered by the atmosphere, and illuminates "shaded" areas, although the illumination is typically much less than that from direct beam.

The brightness of a cell depends on the local incidence angle, the angle between the incoming light ray and the surface normal, shown as θ in Figure 11-29. The surface normal is defined as a line perpendicular to the local surface. Direct beam sunlight striking

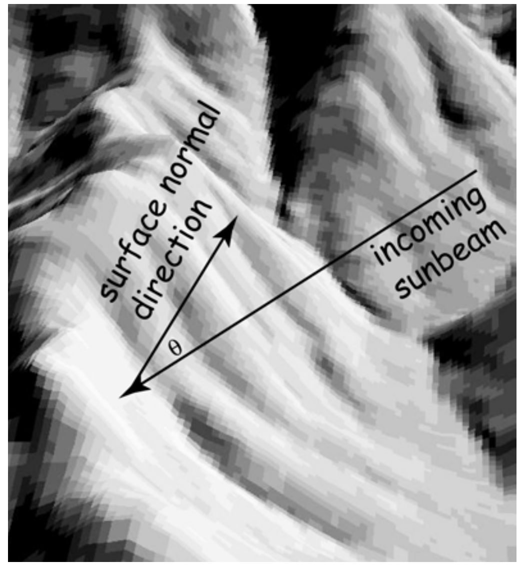

Figure 11-29: Hillshade maps show reflectance as a function of the angle, θ, between sunbeams and surface normals.

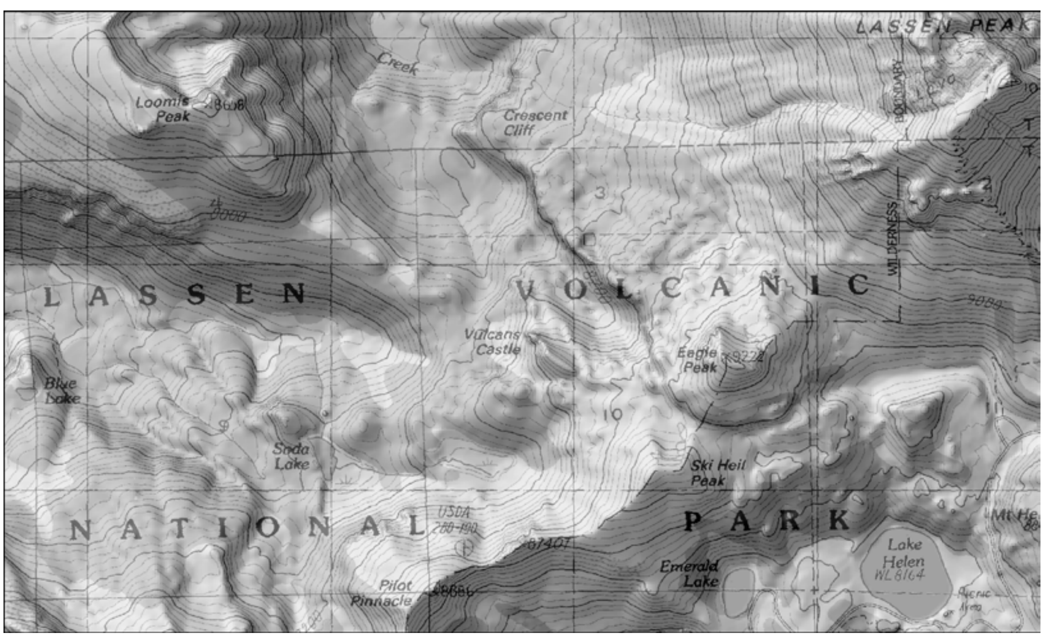

Figure 11-28: Relief shading is often added as a background "under" other mapped data to provide a sense of terrain shape and steepness. This shading provides a three-dimensional perspective for a mapped area, as demonstrated in this relief shading of a U.S. Geological Survey 1:24,000 scale quandrangle map.

the surface at a right angle (θ = 0) provides the brightest return, and hence appears light. As θ increases, the angle between the direct beam and the ground surface deviates from perpendicular, and the brightness decreases. Diffuse sunlight alone provides a relatively weak return, and hence appears dark. Combinations of direct and diffuse light result in a range of gray shades, and this range depends on the terrain slope and angle relative to the sun's location. Hence, subtle variations in terrain are visible on shaded relief maps.

Calculating a shaded relief surface requires specifying the sun's position, usually via the solar zenith angle, measured from vertical down to the sun's location, and the solar azimuth angle, measured from north clockwise to the sun's position (Figure 11-30). Local slope and surface azimuth define a surface normal direction. An angle may be defined between the solar direction and the surface normal direction, shown as θ in Figure 11-30. As noted earlier, the amount of reflected energy decreases as θ increases,

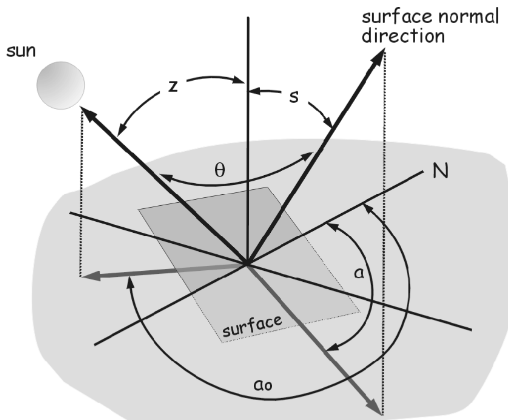

incidence angle θ is equal to:

$$\cos^{-1}[\cos(z)\cos(s) + \sin(z)\sin(s)\cos(a_o - a)]$$

where: z is the solar zenith angle
a_o is the solar azimuth angle
s is the surface normal slope angle
a is the surface normal azimuth angle

Figure 11-30: Direct beam reflectance may be calculated as shown above from the incidence angle, θ, between the incoming sunbeam and the local surface normal. The surface normal is defined by a line perpendicular to the local surface plane.

and this may be shown as various shades of grey in a hillshade surface.

A shaded relief map also requires a calculation of visibility, often prior to calculating the reflectances. Visibility to the sun is determined; if a cell is visible from the sun, the slope and aspect values are used to assign the cell brightness.

Terrain Analysis Software

Terrain analysis and DEM data management and analysis are important enough to be included in most general-purpose GIS packages, including ArcGIS, GRASS, ERDAS, Idrisi, and Manifold. While they support the most common set of terrain and hydrologic analyses, none of these packages includes the broadest range of terrain processing and analysis functions. Specialized analyses are often performed using software with a specific focus on terrain analysis. These include the Whitebox GAT, from the University of Guelph, and commercial tools, such as the Watershed Modeling System (WMS) by the Scientific Software Group.

Whitebox GAT contains what is likely the most comprehensive set of terrain analysis functions in a freely available package. Support is particularly strong for hydrologic surface and stream link processing and analysis, with functions for calculating various flow direction, accumulation, and watershed delineation methods typically not supported by other packages. Basic terrain modification, LiDAR data input and processing, and general raster GIS functions are also supported.

Landserf is a package with particularly strong support for terrain shape and geomorphological analysis, in addition to a strong focus on surface visualization. Multiple methods of calculating and combining first- and second-order terrain gradients are supported, as well as basic elevation data conversion and processing. Landserf is written in Java, and hence available across the widest range of operating systems.

ArcHydro is a set of hydrologic analysis tools written as an extension to ArcGIS. It supports a fairly complete set of hydrologic and watershed delineation functions.

There are many other packages available, including RiverTools, TAUDEM, Surfer, TAPES, and MicroDEM, which provide various specialized capabilities, and may be worth investigating for users interested in terrain and hydrologic analysis.

Summary

Terrain analyses are commonly performed within the framework of a GIS. These analyses are important because terrain governs where and how much water will accumulate on the landscape, how much sunlight a site receives, and the visibility of human activities.

Slope and aspect are two of the most used terrain variables. Both are commonly calculated via trigonometric functions applied in a moving window to a raster DEM. Several kernels have been developed to calculate changes of elevation in x and y directions, and these component gradients are combined to calculate slope and aspect.

Profile curvature and plan curvature are two other important terrain analysis functions. These functions measure the relative convexity or concavity in the terrain, relative to the downslope direction for profile curvature and the cross-slope direction for plan curvature.

Terrain analyses are also used to develop and apply hydrologic functions and models. Watershed boundaries, flow directions, flowpaths, and drainage networks may all be defined from digital elevation data.

Viewsheds are another commonly applied terrain analysis function. Intervisibility may be computed from any location on a DEM. A line of sight may be drawn from any point to any other point, and if there is no intervening terrain, then the two points are intervisible. Viewsheds are often used to analyze the visibility of landscape alterations or additions, for example, when siting new roads, powerlines, or large buildings.

Finally, relief shading is another common use of terrain data. A shaded relief map is among the most effective ways to depict terrain. Terrain shading is often derived from DEMs and depicted on maps.

Suggested Reading

Ali, G., Birkel, C., Tetzlaff, D., Soulsby, C., McDonnell, J.J., Tarolli, P. (2014). A comparison of wetness indices for the prediction of observed connected saturated areas under contrasting conditions. *Earth Surface Process and Landforms*, 39:399–413.

Ayeni, O.O. (1982). Optimum sampling for digital terrain models. *Photogrammetric Engineering and Remote Sensing*, 48:1687–1694.

Band, L.E. (1986). Topographic partition of watersheds with digital elevation models. *Water Resources Research*, 22:15–24.

Baral, D.J., Gupta, R.P. (1997). Integration of satellite sensor data with DEM for the study of snow cover distribution and depletion patterns. *International Journal of Remote Sensing*, 18:3889–3894.

Berry, J.K. (1986). A mathematical structure for analyzing maps. *Environmental Management*, 11:317–325.

Berry, J.K. (1987). Fundamental operations in computer-assisted mapping. *International Journal of Geographic Information Systems*, 1:119–136.

Beven, K.J., Kirby, M.J. (1979). A physically-based variable contributing area model of basin hydrology. *Hydrological Sciences Bulletin*, 24:43–69.

Bolstad, P.V., Stowe,T. (1994). An evaluation of DEM accuracy: elevation, slope and aspect. *Photogrammetric Engineering and Remote Sensing*, 60:1327–1332.

Bonham-Carter, G.F., (1996). *Geographic Information Systems for Geoscientists: Modelling with GIS*. Ottawa: Pergamon.

Burrough, P.A., McDonnell, R.A. (1998). *Principles of Geographical Information Systems* (2nd ed.). New York: Oxford University Press.

Collins, S.H., Moon, G.C. (1981). Algorithms for dense digital terrain models. *Photogrammetric Engineering and Remote Sensing*, 47:71–76.

DeFloriani, L., Magillo, P. (1994). Visibility algorithms on triangulated digital terrain models. *International Journal of Geographical Information Systems*, 8:13–41.

Dozier, J., Frew, J. (1990). Rapid calculation of terrain parameters for radiation modeling from digital elevation data. *IEEE Transactions on Geoscience and Remote Sensing*, 28:963–969.

Dubayah, R., Rich, P.M. (1995). Topographic solar radiation models for GIS. *International Journal of Geographical Information Systems*, 9:405–419.

Fisher, P.F. (1996). Reconsideration of the viewshed function in terrain modeling. *Geographical Systems*, 3:33–58.

Flint, A.L., Childs, S.W. (1987). Calculation of solar radiation in mountainous terrain. *Agricultural and Forest Meteorology*, 40:233–249.

Hengl, T., Reuter, H.I., Eds. (2009). *Geomorphometry: Concepts, Software, Applications*. Amsterdam: Elsevier.

Hodgson, M.E. (1995). What cell size does the computed slope/aspect angle represent? *Photogrammetric Engineering and Remote Sensing*, 61:513–517.

Horn, B.K. (1981). Hill shading and the reflectance map. *IEEE Proceedings on Geosciences*, 69:14–47.

Hutchinson, M.F. (1989). A new procedure for gridding elevation and stream line data with automatic removal of spurious pits. *Journal of Hydrology*, 106:211–232.

Hutchinson, M.F. (1993). Development of a continent-wide DEM with applications to terrain and climate analysis, In: M.F. Goodchild et al. (Eds.). *Environmental Modeling with GIS*. New York: Oxford University Press.

Jain, M.K., Kothyari, U.C., & Ranga, R.K.G. (2004). A GIS based distributed rainfall-runoff model. *Journal of Hydrology*, 299:105–122.

Jenson, S.K. (1991). Applications of hydrologic information automatically extracted from digital elevation models. *Hydrologic Processes*, 5:31–44.

Jenson, S.K., Domingue, J.O. (1988). Extracting topographic structure from digital elevation data for geographic information system analysis. *Photogrammetric Engineering and Remote Sensing*, 54:1593–1600.

Jones, N.L., Wright, S.G., Maidment, D.R. (1990). Watershed delineation with triangle-based terrain models. *Journal of Hydraulic Engineering*, 116:1232–1251.

Julian, J.P., Elmore, A.J., Guinn, S.M. (2012). Channel head locations in forested watersheds across the mid-Atlantic United States: A physiographic analysis. *Geomorphology*, 177/78:194–203.

Lindsay, J.B. (2005). The terrain analysis system: a tool for hydro-geomorphic applications. *Hydrological Processes*, 19:1123–1130.

Lindsay J.B. (2016). The practice of DEM stream burning revisited. *Earth Surface Processes and Landforms*, 41(5): 658-668. DOI: 10.1002/esp.3888.

Louhaichi, M., Borman, M.M., Johnson, A.L., Johnson, D.E. (2003). Creating low-cost high-resolution digital elevation models. *Journal of Range Management*, 56:92–96.

Martz, L.W., Garbrecht, J. (1998). The treatment of flat areas and depressions in automated drainage analysis of raster digital elevation models. *Hydrological Processes*, 12:843–856.

Maune, D.F. (Ed.). (2007). *Digital Elevation Model Technologies and Applications: The DEM User's Manual* (2nd ed.). Bethesda: American Society of Photogrammetry and Remote Sensing.

Moore, I.D., Grayson, R.B. (1991). Terrain-based catchment partitioning and runoff prediction using vector elevation data. *Water Resources Research*, 27:1177–1191.

Moore, I.D., Turner, A, Jenson, S., Band, L. (1993). GIS and land surface-subsurface process modelling, In M.F. Goodchild et al. (Eds.), *Environmental Modeling with GIS*. New York: Oxford University Press.

Skidmore, A.K. (1989). A comparison of techniques for calculating gradient and aspect from a gridded digital elevation model. *International Journal of Geographical Information System*s, 3:323–334.

Southee, F.M., Treitz, P.M., Scott, N.A. (2012). Application of LiDAR terrain surfaces for soil moisture modeling. *Photogrammetric Engineering and Remote Sensing*, 12:1241–1251.

Strahler, A.N. (1957). Quantitative analysis of watershed geomorphology, *Transactions of the American Geophysical Union*, 8:913–920.

Tarboton, D.G., Bras, R.L., Rodriguez-Iturbe, I. (1992). A new method for the determination of flow directions and upslope areas in grid digital elevation models. *Water Resources Research*, 33:309–319.

Tomlin, C.D. (1990). *Geographic Information Systems and Cartographic Modeling*. Upper Saddle River: Prentice-Hall.

Wilson, J.P. (2012). Digital terrain modeling. *Geomorphology*, 137:107–121.

Wilson, J., Gallant, J. (Eds.). (2000). *Terrain Analysis: Principles and Applications*. New York: Wiley.

Wood, J. (1996). The geomorphological characterization of digital elevation models. Ph.D. thesis, University of Leicester, UK.

Wood, R., Sivapalan, M., Robinson, J. (1997). Modeling the spatial variability of surface runoff using a topographic index. *Water Resources Research*, 33:1061–1073.

Zevenbergen, L.W., Thorne, C.R. (1987). Quantative analysis of land surface topography. *Earth Surface Processes and Landforms*, 12:47–56.

Zhou, Q., Liu, X. (2004). Analysis of errors of derived slope and aspect related to DEM data properties. *Computers & Geosciences,* 30:369–378.

Ziadat, F.M. (2005). Analyzing digital terrain attributes to predict soil attributes for a relatively large area. S*oil Science Society of America Journal*, 69:1590–1599.

Study Questions

11.1 - What are digital elevation models, and why are they used so often in spatial analyses?

11.2 - How are digital elevation data created?

11.3 - Write the definition of slope and aspect, and the mathematical formulas used to derive them from digital elevation data.

11.4 - Calculate dZ/dx and dZ/dy for the following 3 x 3 windows. Elevations and the cell dimension are in meters.

windows | 4-nearest cell | 3rd-order finite difference

a)

110	113	118
112	114	119
111	117	121

←10→

4-nearest cell: dZ/dx = , dZ/dy=

3rd-order finite difference: dZ/dx = , dZ/dy =

b)

67	63	62
65	64	64
70	68	66

4-nearest cell: dZ/dx = , dZ/dy=

3rd-order finite difference: dZ/dx = , dZ/dy =

c)

18	23	17
21	24	19
20	22	18

4-nearest cell: dZ/dx = , dZ/dy=

3rd-order finite difference: dZ/dx = , dZ/dy =

11.5 - Calculate dZ/dx and dZ/dy for the following 3 x 3 windows. Elevations and the cell dimension are in meters.

windows	4-nearest cell	3rd-order finite difference

a)

108	112	115
119	116	118
113	118	119

←10→

4-nearest cell: dZ/dx =

dZ/dy=

3rd-order finite difference: dZ/dx =

dZ/dy =

b)

68	63	61
69	67	66
70	71	72

4-nearest cell: dZ/dx =

dZ/dy=

3rd-order finite difference: dZ/dx =

dZ/dy =

c)

15	19	18
19	20	19
21	23	24

4-nearest cell: dZ/dx =

dZ/dy=

3rd-order finite difference: dZ/dx =

dZ/dy =

11.6 - Calculate the slope and aspect for the underlined cell values, using the four nearest cell method.

712	709	707	703	704
710	<u>706</u>	704	700	702
708	705	705	<u>697</u>	700
711	<u>709</u>	705	696	694
714	712	708	703	698

←10→

11.7 - Calculate the slope and aspect for the underlined cell values, using the four nearest cell method.

712	709	707	703	704
710	706	704	a) 700	702
708	705	b) 705	697	700
711	709	705	c) 696	694
714	712	708	703	698

←20→

11.8 - Calculate the slope and aspect for the underlined cell values, using the third-order finite difference method.

712	709	707	703	704
710	706	704	700	702
708	705	705	697	700
711	709	705	696	694
714	712	708	703	698

←10→

11.9 - Calculate the slope and aspect for the underlined cell values, using the third-order finite difference method.

712	709	707	703	704
710	706	704	a) 700	702
708	705	b) 705	697	700
711	709	705	c) 696	694
714	712	708	703	698

←20→

11.10 - Plot a graph of slope in degrees (on x axis) against slope in percent (y axis). Which is usually larger, slope as degrees, or slope expressed as percent?

11.11 - What is an elevation contour?

11.12 - Draw the approximate location of contours for the following set of points. Start contours at the 960 value and use a 30 unit contour interval. For this exercise, it is permissible to estimate the contour locations visually; you do not have to calculate the distances between points to place the contour lines.

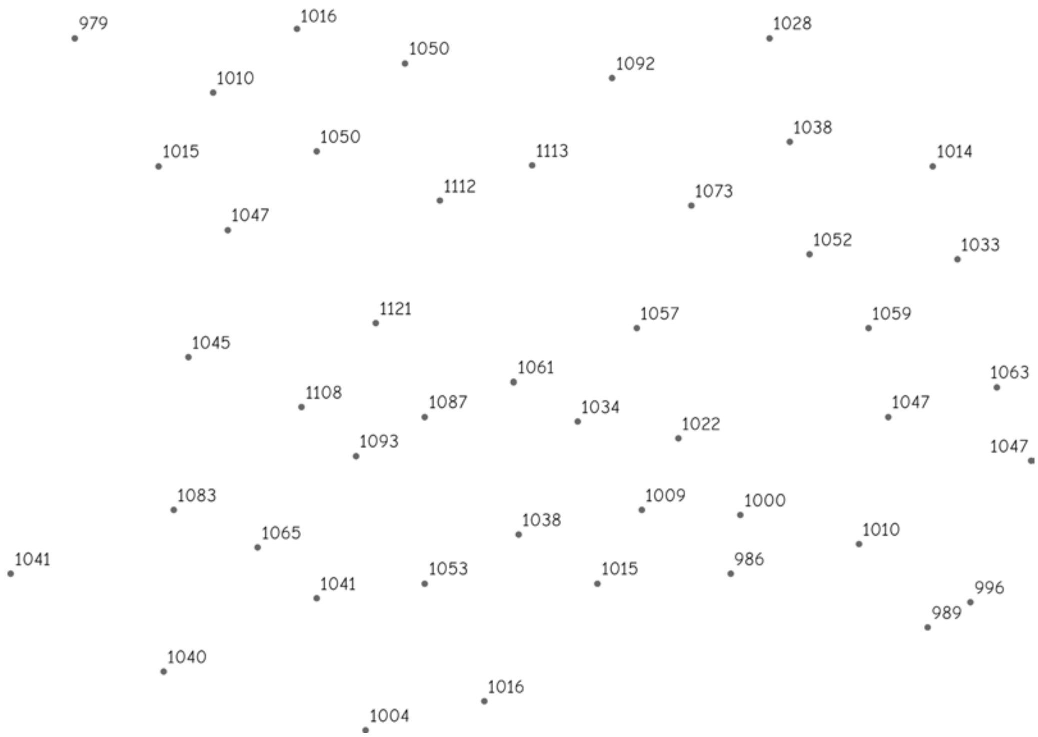

11.13 - Draw the approximate location of contours for the following set of points. Start contours at the 0 value and use a 200 unit contour interval. For this exercise, it is permissible to estimate the contour locations visually; you do not have to calculate the distances between points to place the contour lines.

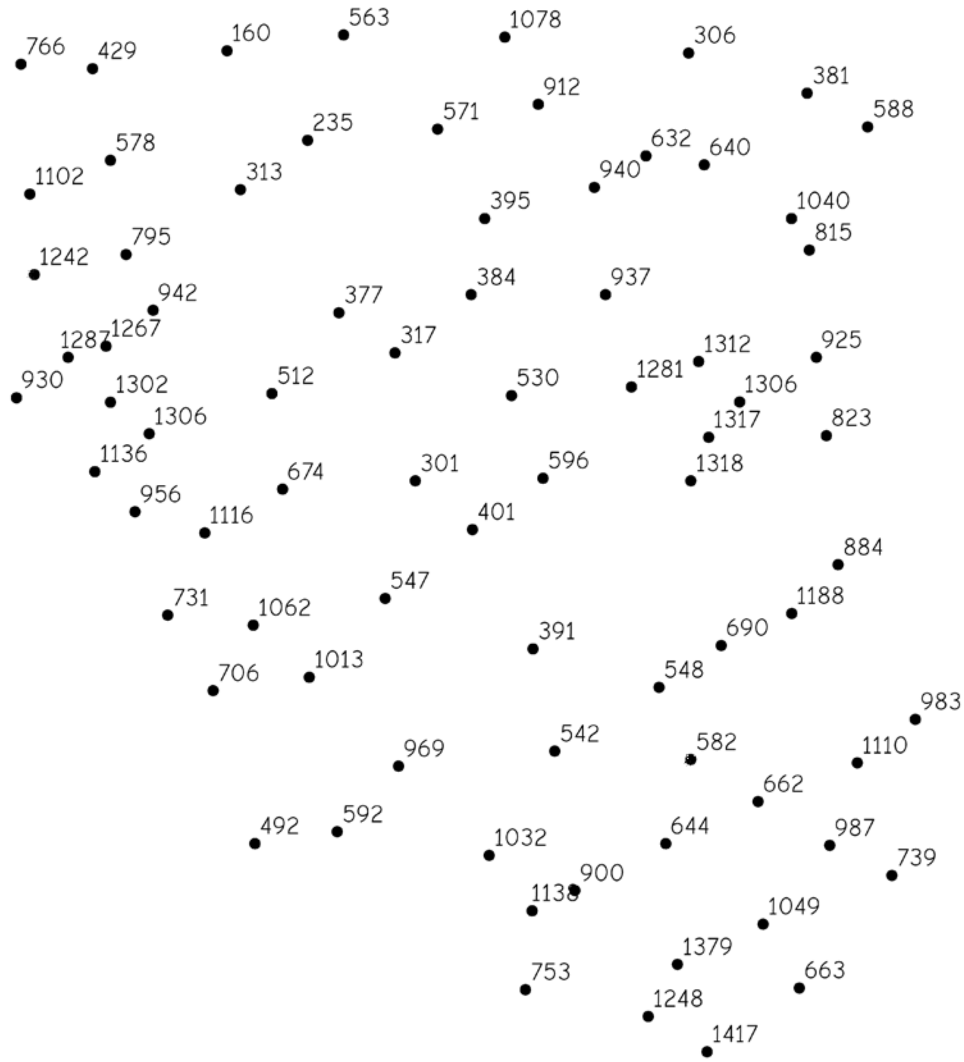

11.14 - What is the formula to calculate a contour height from two measured elevations?

11.15 - Using the figure below, calculate the distances to the listed contour line along the shortest path between points. The example shows the distance calculation from Point A to the contour with value 250, along the straight line from A to B, when the values of A and B are shown, and the distance from A to B is 148.

Distance from B to the 300 contour on the line B - D, when d_{BD} is 94

Distance from E to the 250 contour on the line E - D, when d_{ED} is 115

Distance from C to the 200 contour on the line C - D, when d_{CD} is 188

Distance from E to the 300 contour on the line E - G, when d_{EG} is 248

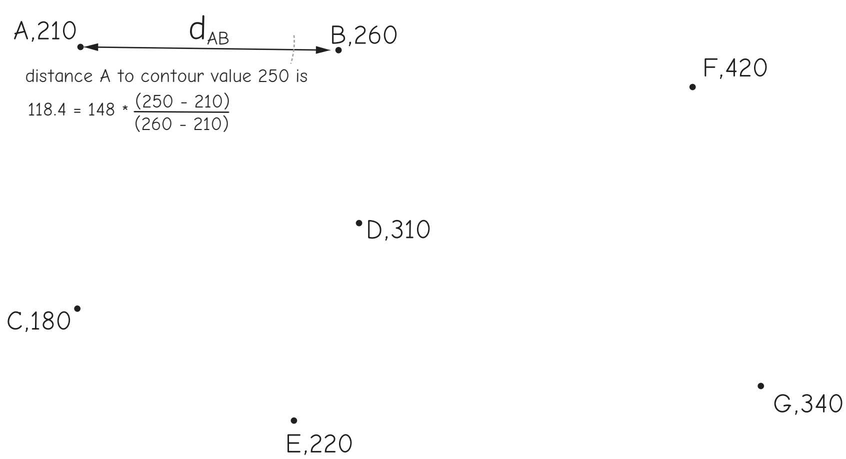

11.16 - Using the figure above, answer the following:

Distance from A to the 200 contour on the line A - C, when d_{AC} is 94

Distance from E to the 300 contour on the line E - D, when d_{AC} is 115

Distance from F to the 400 contour on the line F - G, when d_{FG} is 178

Distance from B to the 350 contour on the line B - F, when d_{BF} is 224

Distance from E to the 250 contour on the line E - G, when d_{EG} is 248

11.17 - What are the plan curvature and profile curvature, and how do they differ?

11.18 - Define the watershed boundaries and possible stream locations in the digital elevation data depicted below:

373	366	369	383	378	356	337	329	328	326	327	326	331	338	330	322	322	314	301	293
384	380	384	392	380	357	343	339	340	341	342	343	346	350	343	335	327	312	303	304
409	405	405	401	380	360	354	356	361	362	359	356	354	352	349	345	336	320	316	322
420	417	416	407	384	367	368	375	376	369	357	345	337	332	332	335	336	327	321	323
399	397	401	399	379	362	367	381	381	365	344	327	317	312	312	320	328	323	313	310
369	369	377	381	366	349	353	370	378	366	343	324	310	300	301	315	328	320	306	300
355	353	362	370	359	340	338	357	372	365	344	324	305	293	296	315	329	319	298	288
349	343	348	359	351	332	327	342	358	357	341	318	295	285	292	310	322	313	292	278
343	333	336	348	338	318	313	323	341	349	335	309	283	275	282	298	310	301	282	270
336	323	326	336	324	304	297	305	326	339	329	302	275	265	270	285	298	291	271	260
322	309	308	321	316	297	283	289	309	325	322	299	271	256	260	274	286	281	262	249
308	295	292	309	314	295	275	273	288	303	302	286	265	250	250	260	266	263	249	240
298	287	281	295	305	293	273	262	269	277	274	264	253	242	239	242	245	244	238	233
282	275	269	275	283	281	269	257	254	255	251	244	238	234	231	231	232	232	229	228
278	275	270	265	264	264	262	257	252	245	240	238	237	236	235	234	234	233	229	225
303	299	289	274	266	262	257	256	252	246	246	251	253	252	250	249	248	244	236	228
322	313	296	280	278	276	265	257	251	249	261	272	273	273	271	271	267	259	247	234
321	308	290	279	285	287	276	265	253	252	269	282	284	284	284	285	280	268	253	238

11.19 - Define the watershed boundaries and possible stream locations in the digital elevation data depicted below:

162	108	67	103	56	66	130	214	153	122	70	36	56	91	165
169	160	101	120	95	115	119	202	212	121	55	43	101	158	261
254	224	182	158	214	142	208	249	225	129	58	121	137	253	344
323	312	204	191	214	228	300	345	195	126	58	105	188	298	381
338	334	267	307	231	194	200	190	176	114	63	141	199	277	278
438	471	405	344	228	242	194	137	103	81	111	103	198	262	195
550	550	387	304	301	330	245	257	175	110	163	204	225	206	144
669	557	502	414	451	378	396	329	180	148	242	349	293	191	148
604	639	490	442	433	425	406	264	169	169	278	401	297	241	167
742	666	536	443	340	294	265	202	221	227	339	342	260	260	245
799	630	509	438	456	414	304	344	337	322	359	377	387	375	308
767	685	608	578	457	426	318	442	371	421	430	330	275	292	226
734	789	721	578	512	421	443	512	506	503	378	315	227	213	173
668	765	826	728	579	558	489	534	513	366	330	244	266	190	170
705	767	784	785	761	675	607	545	440	275	226	202	165	104	55

11.20 - Define the following: solar zenith angle, solar azimuth angle, and solar incidence angle.

11.21 - Draw a diagram illustrating the solar incidence angle, and identify what site/terrain factors affect the solar incidence angle.

11.22 - What are viewsheds, when are they used, and how are they calculated?

11.23 - What is a shaded relief map? How are the values for each cell of a hillshade surface calculated?